

Supplementary Material for “Wavelet-based wavenumber spectral estimate of eddy kinetic energy: Application to the North Atlantic”

Takaya Uchida^{a,b*}, Quentin Jamet^{c,d}, Andrew Poje^e, Nico Wienders^a & William Dewar^{b,f}

a: *Center for Ocean-Atmospheric Prediction Studies, Florida State University*

b: *Université Grenoble Alpes, CNRS, INRAE, IRD, Grenoble INP, IGE*

c: *Service Hydrographique et Océanographique de la Marine*

d: *Institut National de Recherche en sciences et technologies du numérique, ODYSSEY group, Ifremer*

e: *Department of Mathematics, College of Staten Island, The City University of New York*

f: *Department of Earth, Ocean and Atmospheric Science, Florida State University*

*Will be moving to the *Climate Dynamics Laboratory, МФТИ, Россия.*

Table of Contents:

- Figures S1, S2, S3 and S4.

In this document, we display the frequency spectra of total kinetic energy at a model grid point closest to where mooring data from Line W (<https://hdl.handle.net/1912/28669>; 39.6° N/69.7°E, and 2, 180-m depth) were publicly available between 2004–2007 in the path of the Deep Western Boundary Current. We first concatenate the four years of data into a single time series and then take a running five-day averaging of the mooring data to remove tidal signals and to be consistent with our five-day averaged model outputs (Jamet et al., 2019b). Missing data were interpolated over with a first-order spline and the time series were linearly detrended. Our ensemble misses the variability at the tail ends of frequency but captures the local maximum around frequencies corresponding to 30–50 days, which is likely associated with the abyssal eddies decomposed about the ensemble mean (Fig. S1).

We also provide preliminary findings from a partially air-sea coupled 1/50° ensemble of the separated Gulf Stream region. We currently have 48 members spun up where each ensemble member was spun up for a year with cyclic atmospheric and lateral boundary conditions of 2003. The cyclic external conditions were constructed by patching together the time series in late June 2003 and early July 2002, and linearly interpolating between them in time. The atmospheric states were taken from Drakkar Forcing Set (DFS) 4.4, identical to Jamet et al. (2019a), and lateral boundary conditions were taken from the 48-member 1/12° Chaocean dataset, which were used in the main text of the manuscript. The initial conditions on January 1, 2003 for the 1/50° ensemble were also taken from Chaocean. All three (i.e. atmospheric, boundary and initial) conditions were spatially interpolated down to 1/50°. The atmospheric

states were updated every six hours and lateral boundary conditions every five days to force the ensemble. Namely, each ensemble member sees the same atmosphere above the atmospheric boundary layer but differs in their initial and lateral boundary conditions, which have corresponding Chaocean realizations. Other than numerical viscosity, bottom drag, and bathymetry, the new ensemble configuration was kept identical to Chaocean. Such decisions were made so as to be able to make direct comparisons between the $1/12^\circ$ and $1/50^\circ$ ensembles upon production. Bathymetry was constructed by interpolating the 15 arc-second GEBCO bathymetry onto our model grid and then a Gaussian smoothing with the standard deviation of three kilometers was applied two times using the `gcm-filters` Python package (Grooms et al., 2021) in order to alleviate pressure gradient errors. Below, we provide figures showing the surface relative vorticity $\zeta = v_x - u_y$ from an arbitrary ensemble member (Fig. S2) and wavenumber spectra of eddy kinetic energy (EKE) in the separated Gulf Stream and quiescent gyre-interior region (Fig. S3) on the last day of spin up. The $\mathcal{O}(1)$ local Rossby numbers in the separated Gulf Stream imply that there is a loss of balance from geostrophy.

In addition to the instantaneous snapshot outputs saved every five days, five-day averaged outputs were also saved during the Chaocean ensemble production. Figure S4 shows the spatially-filtered horizontal spectral flux of total (eddy+mean) KE at 120 km length scale using instantaneous snapshots (left) and five-day averaged outputs (right). We find that using temporally averaged outputs leads to a diminishing signal in the forward cascade; unbalanced motions, which drive the forward cascade, get smoothed out with a time averaging. Because the spectral flux of KE is a nonlinear term, the order of applying time averaging is non-commutable. Namely, $\langle S_l(\overline{u}^t); \mathbf{T}_l(\overline{u}^t, \overline{u}^t) \rangle \neq \overline{\langle S_l(u); \mathbf{T}_l(u, u) \rangle}^t$ where $\overline{(\cdot)}^t$ is the time-averaging operator. The right panel in Fig. S4 has more regions with an inverse cascade.

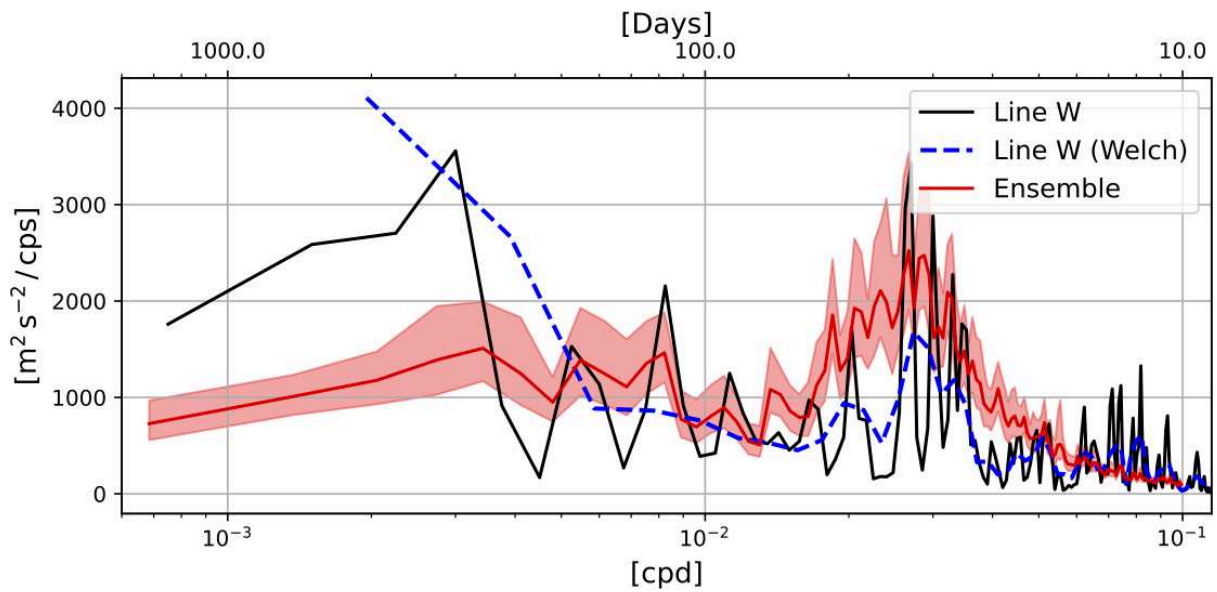


FIGURE S1: Fourier frequency spectra of total kinetic energy taken from the Line W mooring data and our Chaocean 48-member ensemble. The Line-W spectra are shown as a periodogram (black solid) and when Welch's method is applied (blue dashed). The 95% bootstrapped confidence interval is given for our ensemble spectrum in red shading. A linear trend was removed and the Hann window was applied to make each time series periodic. The fast Fourier transform (FFT) method (and not wavelet) was chosen here as we are interested in the frequency signals over the entire time series and not localized about any specific time.

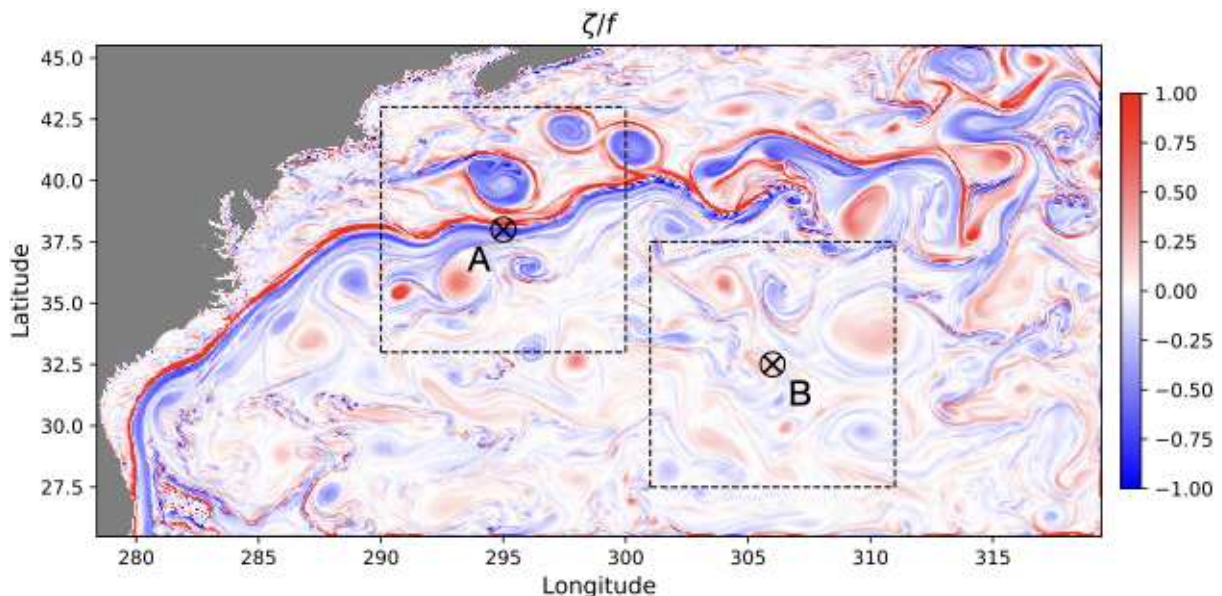


FIGURE S2: Surface relative vorticity normalized by the Coriolis frequency (i.e. the local Rossby number) from member 31 is shown for the entire $1/50^\circ$ model domain on Jan. 1, 2003, the last day of spin up. The black dashed lines indicate the subdomains A and B over which the wavenumber spectra were computed (Fig. S3).

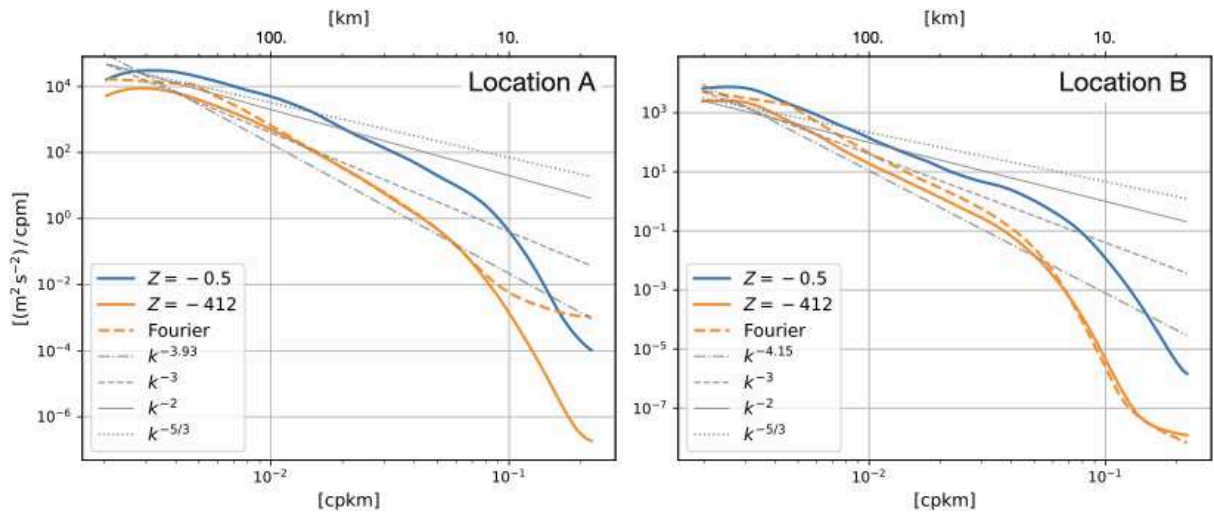


FIGURE S3: Isotropic wavelet wavenumber spectra of EKE are shown in solid curves for $z = -0.5, -412$ m while the Fourier spectrum is shown in the orange dashed curve for $z = -412$ m. The wavelet spectra are taken at the center of the subdomains shown by \otimes in Fig. S2. Scaling laws predicted by inertial-range arguments are indicated by the grey dashed and dotted lines and a least-squares fit between the scales of 200–20 km for $z = -412$ m is shown in the grey dash-dotted line with a slope of -3.93 and -4.15 for location A and B respectively. At location A, the spectrum shoals significantly at scales larger than 100 km, exhibiting a -2 scaling law (grey solid line) at the surface. The scaling law is closer to -3 at location B at the surface.

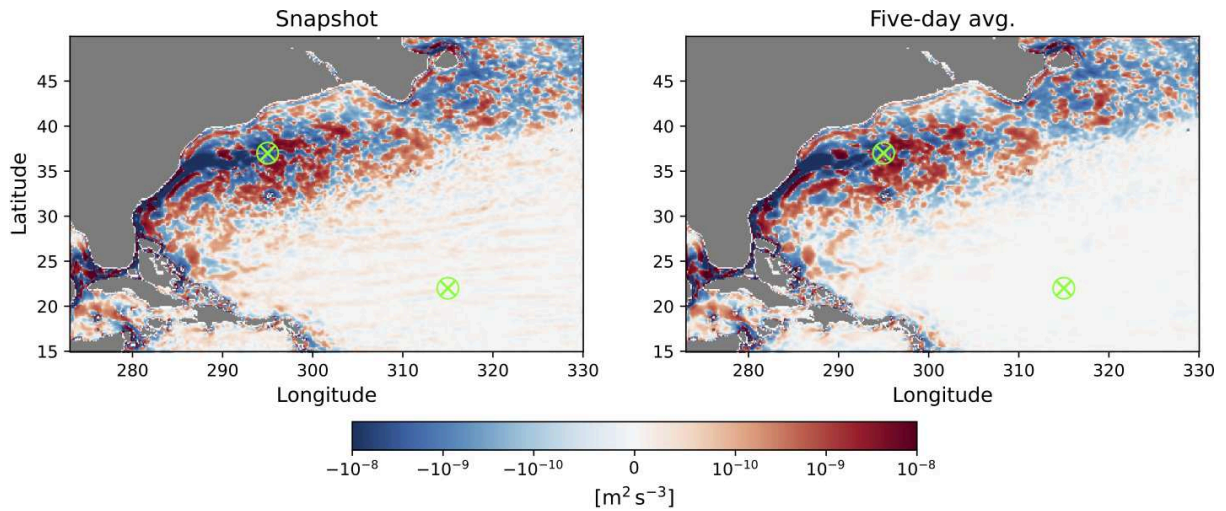


FIGURE S4: Annual mean of horizontal spectral flux computed by spatially filtering total horizontal momentum $\langle S_l(u); \mathbf{T}_l(u, u) \rangle = \langle (\overline{uu}^l - \overline{u}^l \overline{u}^l) \overline{u}_x^l + (\overline{uv}^l - \overline{u}^l \overline{v}^l) (\overline{u}_y^l + \overline{v}_x^l) + (\overline{vv}^l - \overline{v}^l \overline{v}^l) \overline{v}_y^l \rangle$ every 15 days at $z = -452$ m from the Chaocean ensemble. We show the annual-mean flux corresponding to the length scale of 120 km using instantaneous (left) and five-day averaged outputs (right). Locations A and B in the main text of the manuscript are denoted by the lime-colored \otimes .

References

- Grooms, I., N. Loose, R.P. Abernathey, J.M. Steinberg, S.D. Bachman, G. Marques, A.P. Guillaumin & E. Yankovsky. (2021). Diffusion-based smoothers for spatial filtering of gridded geophysical data. *J. Adv. Model. Earth Syst.*, doi:10.1029/2021MS002552.
- Jamet, Q., W.K. Dewar, N. Wienders & B. Deremble. (2019a). Fast warming of the surface ocean under a climatological scenario. *Geophys. Res. Lett.*, doi:10.1029/2019GL082336.
- Jamet, Q., W.K. Dewar, N. Wienders & B. Deremble. (2019b). Spatio-temporal patterns of chaos in the Atlantic Overturning Circulation. *Geophys. Res. Lett.*, doi:10.1029/2019GL082552.